Computational stochastic modeling of human ventricular myocardium

Ana Pons,* Ariadna Cortés,† and Arnau Marzabal‡
Universitat Politècnica de Catalunya
(Dated: May 31, 2024)

Mathematical models of the action potential of human heart cells have been of great importance in the study of the electrophysiological behaviour of the human ventricular myocardium. In this work, we present the extension of the known Ten Tusscher model to study stochastic evolution via the implementation of binomial gating dynamics, analysing the limits of the commonly used deterministic approach. Also, it is presented the study of the deterministic 1D and 2D tissue simulations calculating propagation speeds and the creation and propagation of spiral waves responsible for reentry arrhythmias, as well as an stochastic 2D tissue simulation. Finally, a pseudo-ECG signal is computed and compared with real ECG signals for reentry tachycardias.

Keywords: Computational biology, electrophysiology, stochastic modeling, spiral waves

I. INTRODUCCTION

Cardiac cell simulation is a pivotal aspect of modern computational biology and medicine, providing profound insights into the complex electrophysiological processes that govern heart function. With cardiovascular diseases remaining the leading cause of mortality worldwide, the need for detailed and accurate models to understand and predict cardiac behavior is crucial. Computational models offer a non-invasive and cost-effective approach to studying cardiac physiology, enabling researchers to explore intricate cellular mechanisms, evaluate drug effects, and develop targeted therapies.

II. TEN TUSSCHER MODEL

Among the various models developed for simulating cardiac cells, the Ten Tusscher model [1] stands out due to its comprehensive and detailed representation of human ventricular dynamics. First introduced by Ten Tusscher and Panfilov in 2006, it has been widely adopted in the field for its ability to replicate the dynamic responses of cardiac cells under various physiological and pathological conditions. This model integrates a total of 13 ion channels that contribute to the action potential of cardiac cells modeling the cell membrane as a capacitor. The dynamics for most of the ion channels follow a Hodgkin-Huxley-type equation [2] while there are other time-independent currents. Hence, the dynamics of the membrane potential can be described by the following differential equation.

$$\frac{dV}{dt} = \frac{I_{Ion} + I_{stim}}{C_m} \tag{1}$$

Where V is the membrane potential, I_{Ion} is the sum of all ionic currents, I_{stim} acts as the stimulation current and

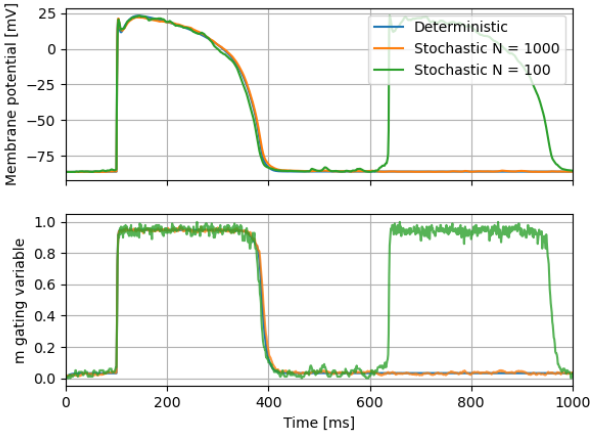

FIG. 1. Membrane potential and Sodium m gate variable evolution for $I_{stim} = -52$ pA/pF during 1 ms at t=100 ms.

C_m stands for the membrane capacitance. In the figure 1 (blue), we have the evolution of the membrane potential and the most important gating variable (m gate) for a normal excitation cycle.

III. SINGLE CELL STOCHASTIC SIMULATION

Most cardiac cell models are sets of first-order differential equations that model the dynamics of the ionic channels. Even though they are an excellent approximation of the general dynamics they lack stochasticity. The real behavior of the ion channels follows a Markov chain, thus for a sufficiently low number of gates this variability could induce spontaneous excitations that would interfere with the normal heart pulses. As a first approximation, we have substituted the gating variables in the Ten Tusscher model with a fraction of open gates which evolve according to the following equation

$$\Delta N_i = Bin(N_{tot} - N_i, \alpha_i(V)\Delta t) - Bin(N_i, \beta_i(V)\Delta t) \tag{2}$$

* ana.pons@estudiantat.upc.edu
† ariadna.cortes.danes@estudiantat.upc.edu
‡ arnau.marzabal@estudiantat.upc.edu

Where N_i represents the number of open gates of type i and N_{tot} is the total number of gates, therefore the ratio N_i/N_{tot} represents the value of the gating variable. Bin stands for binomial distribution and $\alpha_i(V)$ and $\beta_i(V)$ are the rate constants of the $i-th$ channel thus, the first binomial represents the probability for closed gates to open while the second is the probability for the open gates to close in a single time step. For a large number of gates, the results from the deterministic model are recovered since around this limit ($N_{tot} \to \infty$) the effects of the variability of the gates are negligible. We intend to find around which value and for which gates this variability becomes relevant. Figure 1 compares the evolution of a deterministic simulation (blue) against 2 stochastic realizations with $N_{tot} = 1000$ and $N_{tot} = 100$ (orange and green, respectively) where it can be seen that the results for $N_{tot} = 1000$ are virtually the same as the deterministic simulation while the $N_{tot} = 100$ realization exhibits a random excitation around 640 ms. To determine which ion channels are most affected by this stochastic variability, we varied the number of total channels for several channel types.

Considering that there are approximately 50-100 channels per μm^2 and and that a cardiac cell is approximately $100\mu m \times 10\mu m$ we estimate that there are around $10^5 - 10^6$ channels per cell. In our simulations, we set the total number of channels to 10^6 except for only one channel to observe the effect of a reduced number of gates for this specific channel. The simulations revealed that the only channel where the stochasticity becomes relevant is the sodium channel, which for N_{tot} below 400 we start to see some random excitations. This analysis demonstrates that, among the channels studied, the sodium channel exhibits the highest sensitivity to stochastic fluctuations, highlighting its critical role in cardiac stimulation.

Figure 2 illustrates the frequency of stochastic spikes as a function of the total number of sodium channels. We observe that when the number of channels falls below 20, the frequency reaches a limit of 3 Hz due to the impossibility of reexcitation during the refractory period which is around 300 ms.

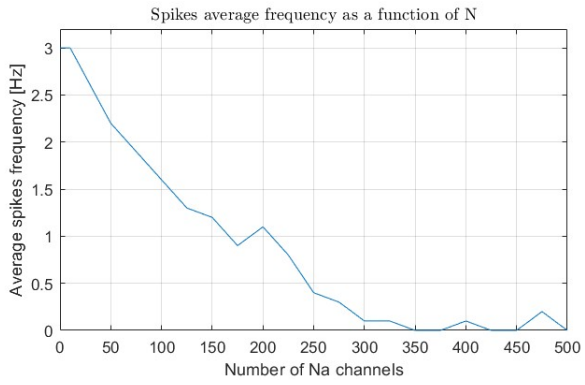

FIG. 2. Stochastic spikes frequency as a function of number of Sodium channels.

IV. TISSUE SIMULATION

As described in the Ten Tusscher model a tissue of cardiac cells can be described by the following partial differential equation

$$\frac{\partial V}{\partial t} = \frac{I_{Ion} + I_{stim}}{C_m} + \frac{1}{\rho S C_m}\nabla^2 V \tag{3}$$

Where ρ is the cellular resistivity and S stands for the surface-to-volume ratio. As suggested by [1], ρ and S were taken such that the diffusion coefficient $D = 1/(\rho S C_m) = 0.00154\ cm^2/ms$. For all the simulations the no flux boundary condition ($\nabla V \cdot \vec{n} = 0$) was applied to all boundaries ensuring charge conservation. In this case, the formulation assumes an isotropic tissue. Although cardiac cells have different sizes in each dimension, this change only becomes relevant when running 3D simulations.

A. 1D simulation

In this section, we present a simplistic analysis of the propagation of the membrane potential wave across a one-dimensional tissue. We can simulate the propagation by externally injecting a current to one end and integrating equation 3 to see the evolution. In this case, we have simulated a 40 cm 1D tissue exciting it with a -52 pA/pF current during 1 ms. Integration time step has been set to $dt = 0.02$ms and the spatial discretization to $dx = 0.02$cm. The plot shown in figure 3 represents the membrane potential at 350ms and 700ms after the excitation at $x = 0$. It is observed the characteristic wave shape for heart action potentials with a potential peak around 20 mV and a long refractory tail of about 13 cm.

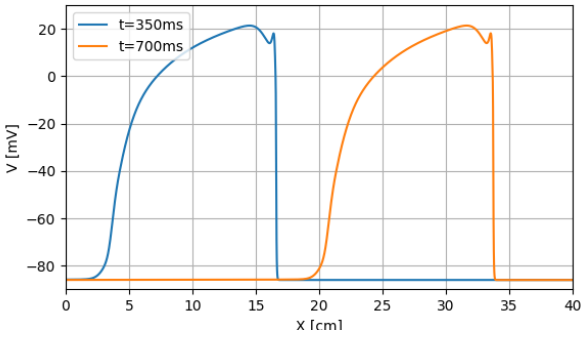

FIG. 3. Membrane potential at $t = 350$ms and $t = 700$ms for 1D simulation of a 40cm tissue and $I_{stim} = -52$ pA/pF.

By measuring the time difference between the peaks of the action potentials in different cells, we calculated the propagation velocity of the electrical signal, which was found to be $v_p = 47$cm/s.

Heart membrane potential waves are characterized by a very long refractory tail, this is, in fact, a safety mechanism since it prevents reexitations of the tissue nearby

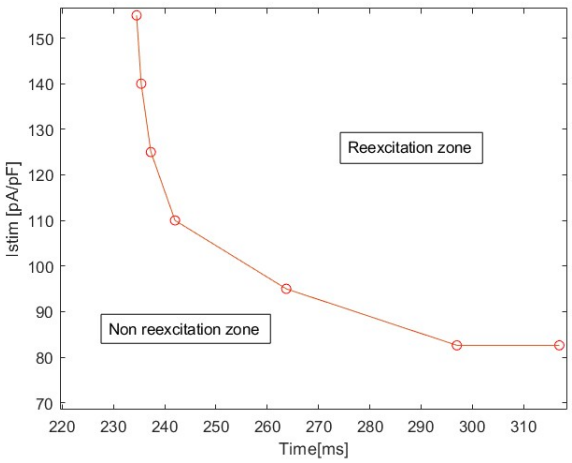

FIG. 4. Phase diagram between intensity-interval pairs that initiate a new wavefront (Reexcitation zone) and those where the stimulation intensity is absorbed by the refractory wave (Non reexcitation zone). I_{Stim} is given in pA/pF while time or interval is the time passed since the first wavefront peak.

an already existing wave. Figure 4 represents the phase diagram for the reexitation wave. The bottom-left zone represents all the intensity-interval pairs that are not able to reexitate the tissue while all pairs in the top-right zone induce the appearance of two new wavefronts. Understanding these transitions helps us study reentry dynamics, which are essential for modeling spiral formations and analysing cardiac arrhythmias.

B. 2D tissue simulation

For a more realistic 2D tissue different phenomena related to the wave propagation can be observed. For instance, reentry arrhythmias are caused by an abnormal excitation on the heart tissue that incites a spiral wave. The rotation frequency of the spiral induces a periodic excitation with a high frequency ($180 - 250$ BPM) thus, giving an arrhythmia.

These spirals can be exited by different protocols, in this case, we used the S1-S2 protocol which consists of stimulating a quadrant of the tissue after the refractory tail of a flat wave has passed a certain point. This second excitation induces a wavefront propagating perpendicular to the initial wavefront with a free end that curls, thus producing the spiral. The interval between the two stimuli is called the S1-S2 interval, in our case 300 ms. Figure 5 shows the membrane potential 75 ms after the S2 stimulation for a 4 cm x 4 cm tissue and figure 6 shows the effect of the second stimulation of the S1-S2 protocol and the creation of the spiral wave. The average period of the spiral was found to be around $291 \pm 10\ ms$. This result was calculated by averaging the frequency of the peaks induced in the ECG signal for a simulation over 1 second (figure 8 bottom).

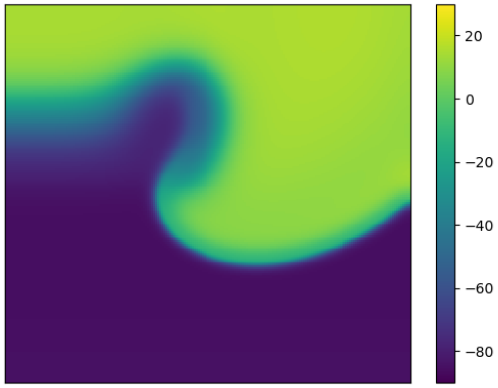

FIG. 5. Membrane potential (mV) during a spiral wave for a 2D-tissue of 4cm x 4cm

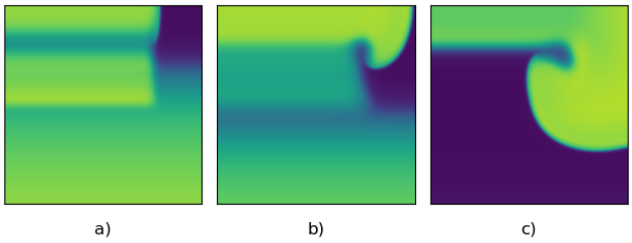

FIG. 6. Graphic representation of the membrane potential during an S1-S2 stimulation protocol and the generation of a spiral wave. Captures a,b and c were taken at $t = 320$, 360 and 400 ms respectively.

C. Stochastic 2D tissue simulation

The stochastic effect observed in a single cell can generate spontaneous stimulations that may succeed in propagating along the cardiac tissue. These so-called restimulations could induce harmful consequences to the normal behavior of the heart. It has been shown that for a reasonable number of gates in the cell, the deterministic approach leads to reliable results. This suggests that while deterministic models are sufficient for predicting overall cell behavior under normal conditions, the stochastic model provides critical information in certain cases. Even though the probabilities of such spontaneous events are low, the heart beats a vast number of times over a person's lifetime, and it can also be susceptible to previous damage. Therefore, the stochastic model is valuable for understanding rare but potentially dangerous events that could impact cardiac health. Employing both deterministic and stochastic models can thus offer a more comprehensive understanding of cardiac behavior, balancing reliability and the ability to predict rare events.

To appreciate this stochastic effects, the number of gates is reduced close to the stochastic limit found in

Section III. It was also shown that the major stochastic effects were observed in the Na channels, since the change probabilities of other gates are negligible in comparison. Figure 7 shows the evolution for a 2D tissue with 50x50 cells with $N_{tot} = 150$ channels. It is shown that for these conditions the stochastic variability is enough to produce spontaneous excitations that could interfere with other spontaneous excitations or standard propagating waves. Also, as a result of the random fluctuations the border of the wavefront becomes blurry (figure 7 b and c).

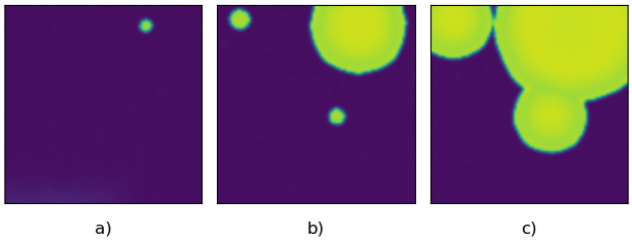

FIG. 7. Evolution of a 2D stochastic tissue simulation with $N_{tot} = 100$

V. VIRTUAL ECG

Another interesting result of these simulations is the capability to reproduce electrocardiograms. A pseudo-ECG ($\phi(r)$) signal at a particular reference point (r) is calculated by integrating over all the dipoles generated by Vm as it propagates across the 2D tissue using the following equation [3].

$$\phi(r) = \int \frac{\nabla^2 V_m(r')}{|r - r'|} d^2 r' \tag{4}$$

By subtracting, the signal of two electrodes one can get a pretty good approximation of a real electrocardiogram signal. Figure 8 shows the ECG signal for a normally stimulated tissue (1cm x 1cm) with a pacing frequency of 60 BPM against the ECG of a wave spiral (reentry arrhythmia). On the normally stimulated tissue, it is easy to identify the typical shape of an ECG with the standard Q,R,S and T waves. P wave does not appear since it is associated with the auricular contraction. The T wave occurs about 300 ms after the Q wave coinciding with the results obtained at section II for the refractory tail. For the arrhythmia ECG it is clear that the frequency is significantly higher (note the change in the time scale).

The shape of the tachycardia ECG has a high resemblance with real tachycardia ECG. Figure 9 shows some ECG signals for different types of tachycardia, and it is easy to see the resemblance between the obtained results and, for example, the last row signal with a bigger R wave followed by a modified S and T waves.

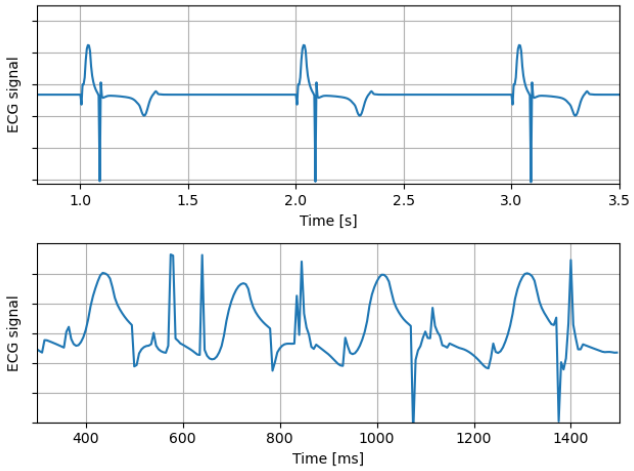

FIG. 8. Comparison between a normal ECG at 60 BPM (top) and a reentry tachycardia ECG (bottom) from a 100x100 lattice

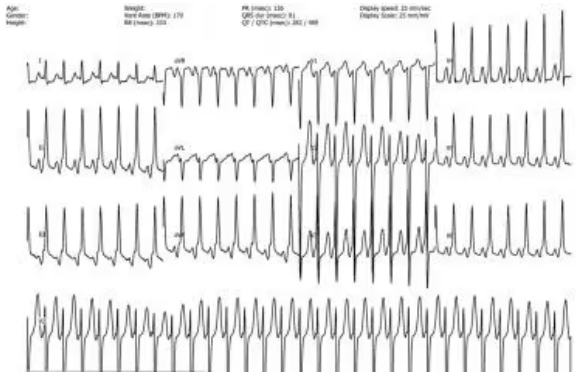

FIG. 9. Real ECG signals for different types of tachycardias [4]

VI. CONCLUSION

In this work, the well-known Ten Tusscher model has been extended to include stochastic effects, and it has been concluded that the random effects of the stochastic are irrelevant for a typical number of gates. Only sodium gates could potentially cause a random excitation for a reduced number of gates, around 400. On the other hand, the simulation of 1D and 2D tissues has been conducted, calculating typical propagation velocities, examining the wave shape and the effects of the refractory tail, and finding the limits of reexitation of the tissue. In addition, a spiral wave in 2D tissue has been studied using the S1-S2 protocol and analyzing its natural frequency. Spontaneous excitations due to stochastic effects on a tissue have been observed and, finally, a virtual ECG signal has been computed for a normally propagated wave and that of a reentry tachycardia produced by the spiral wave, comparing its results with real ECG signals.

REFERENCES

[1] ten Tusscher, K. H., Noble, D., Noble, P. J., & Panfilov, A. V. (2004). "A model for human ventricular tissue." *American Journal of Physiology-Heart and Circulatory Physiology*, 286(4), H1573-H1589.

[2] Hodgkin, A. L., & Huxley, A. F. (1952). "A quantitative description of membrane current and its application to conduction and excitation in nerve." *The Journal of physiology*, 117(4), 500.

[3] Ortiz, J. R., Kaboudian, A., Uzelac, I., Iravanian, S., Cherry, E. M., & Fenton, F. H. (2021, September). "Interactive Simulation of the ECG: Effects of Cell Types, Distributions, Shapes and Duration." In 2021 *Computing in Cardiology (CinC)* (Vol. 48, pp. 1-4). IEEE.

[4] Olshansky, Brian. "Atrioventricular Nodal Reentry Tachycardia Workup: Approach Considerations, Electrocardiography, Electrophysiology." *Emedicine.medscape.com*, 22 July 2022, emedicine.medscape.com/article/160215-workup. Accessed 20 May 2024.

[5] Ten Tusscher, K. H., Bernus, O., & Panfilov, A. V. (2006). "Comparison of electrophysiological models for human ventricular cells and tissues." *Progress in biophysics and molecular biology*, 90(1-3), 326-345.